7

Understanding composite distortion during processing

M R W I S N O M and K D P O T T E R , University of Bristol, UK

7.1   Introduction

Composites distort during manufacture, causing difficulties assembling struc-
tures, and leading to increased costs. An iterative approach to tool design is
often used, with the geometry modified on a trial and error basis in order to
produce the correct cured shape. In this chapter the fundamental mechanisms
that cause the residual stresses producing these distortions are first considered.
The ways in which these mechanisms cause distortion in flat plates and spring-in
in curved composites are then considered, together with the ability of models to
predict the changes in geometry. Finally distortion in more complex structures is
discussed briefly. Much of the research that has been done on this topic has been
for autoclave curing of thermosetting resins, but the same phenomena are
directly relevant to other manufacturing processes.

7.2   Fundamental mechanisms causing residual stresses and distortion

7.2.1   Differential thermal contraction

The expansion coefficient of polymer matrix materials is usually much higher
than that of the fibres. Also the expansion coefficients of many fibres are
orthotropic. For example, carbon fibres have very low or slightly negative
expansion coefficients in the fibre direction, but higher values in the transverse
direction. This leads to residual stresses at the micro-scale during cooldown
even in unidirectional material. Figure 7.1 shows stresses calculated by micro-
mechanical finite element analysis based on a repeating array of fibres for
carbon fibre/epoxy subject to a 100ºC temperature drop.[1] Compressive stresses
are generated along the fibres, with tension in the matrix in the fibre direction.
Hoop tensile stresses arise in the matrix as it shrinks around the fibres. There are
also radial stresses which are compressive where the fibres are close together,
and tensile where they are furthest apart. This produces Von Mises stresses of
nearly 30 MPa in the matrix in this case as a result of the combination of

Von Mises stress   Radial stress

Axial stress   Hoop stress
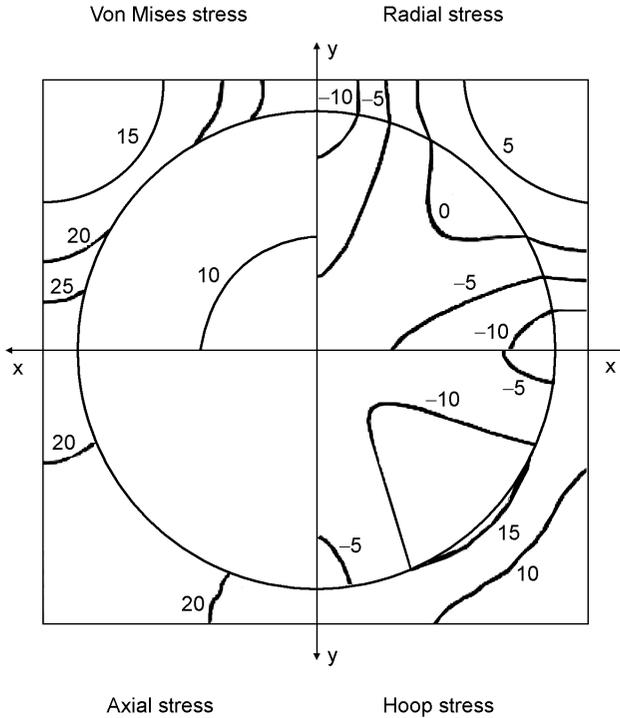
7.1 Residual stresses in carbon-epoxy due to 100°C temperature drop.[1]

stresses, which is a substantial fraction of the strength of the material. These residual stresses can affect the stress-strain behaviour and failure, but do not normally cause distortions because they arise on a very local scale and any distorting effects tend to average out over a larger volume of material.

The second effect is the difference in ply-level expansion coefficients in the fibre and transverse directions that causes in-plane residual stresses in laminates, which can be analysed by classical laminated plate theory. These can lead to distortion in flat plates when lay-ups are not balanced and symmetric.[2] For example, it is well known that unsymmetric cross-ply laminates exhibit curvature, and this is often used to study residual stresses, see, e.g., ref. 3. The presence of angle plies can lead to twist. This mechanism normally only produces significant stresses after vitrification, and is therefore most important on the cooldown after high temperature processing. Close study of unidirectional prepreg shows a significant level of variability in fibre content on a local scale that can generate small differences in distortion between nominally identical laminates.

For components with double curvature, the necessary rearrangements of the reinforcement fibre trajectories to accomodate the geometry in each ply make it very unlikely that the laminate will be balanced and symmetrical at all points

Circumferential stresses in symmetric plies act over same area – no bending

Axial stresses in inner and outer plies act over different areas, causing bending.
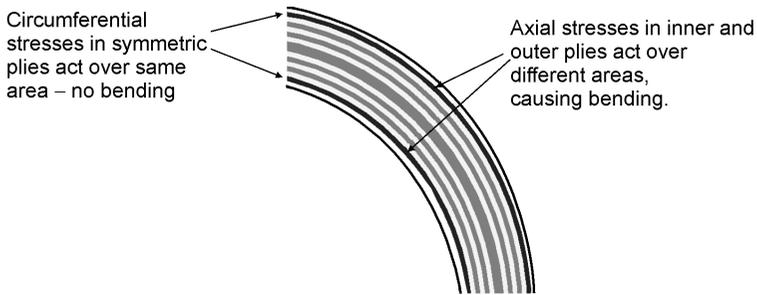
7.2 Pattern of residual stresses normal to plane in a curved balanced symmetric laminate.

across the surface. This lack of symmetry will lead to distortions in the part geometry. To make predictions of these geometrical distortions, thermoelastic and fibre path modelling need to be coupled.

It is less well appreciated that ply-level residual stresses can also produce distortion in curved plates even when the lay-up is balanced and symmetric, due to the effective shift of the neutral axis due to curvature. Figure 7.2 shows the pattern of in-plane residual stresses through the thickness of a balanced symmetric lay-up determined by finite element analysis. The values in this curved section are very similar to those in an equivalent flat lay-up. Consider the two plies shown in dark colour, which have the fibres in the circumferential direction. The circumferential stresses act over the same area, i.e. the ply thickness times the dimension normal to the plane of the figure. Therefore stresses of equal magnitude in the two plies in this direction would not produce any bending. However in the axial direction normal to the section the stresses in the inner ply act over a smaller area than those in the outer ply due to the shorter circumferential length. The forces are no longer in balance with respect to the mid-plane, causing bending and a shift in the neutral axis. This also affects the bending in the other direction, known as spring-in, via the Poisson ratios, although the magnitude is usually small. The same phenomenon causes twist in curved sections with angle plies.[4]

A third effect is the higher through-thickness expansion coefficients (matrix dominated) compared with in-plane values (fibre dominated). This causes a change in curvature of curved laminates with temperature for any lay-up, and is the main origin of the spring-in phenomenon[5] illustrated in Fig. 7.3. This is a geometrical effect that can produce distortions in the absence of large stresses whilst the material is in the rubbery state as well as after vitrification.[6]

7.2.2   Chemical shrinkage

Polymers shrink during the cure producing an additional volume change to that caused by thermal effects. This can be a very substantial effect, with a volume

Original
geometry

Change in
subtended angle
due to through-
thickness
contraction
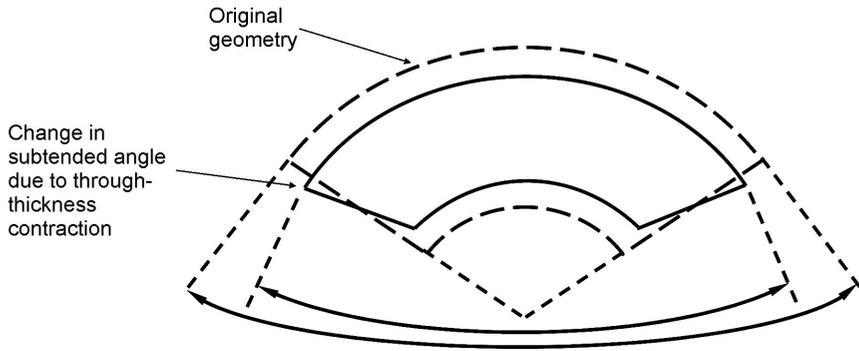
7.3 Illustration of spring-in mechanism.

change of 7% being typical for an epoxy resin.[7] Chemical shrinkage can cause similar effects to thermal contraction, with stresses at the micromechanical level, in-plane stresses and distortions in laminates, and changes in curvature in curved plates. However, for many resins much of the shrinkage occurs before gelation where the material is effectively a liquid. This may be compensated by resin flow, and may cause changes in thickness or volume fraction, adding to consolidation-related geometry changes, but does not directly produce stresses causing distortion. Crystallisation in materials such as PEEK can also cause volume changes leading to residual stresses.[8]

7.2.3   Tool-part interaction

Stresses can arise during the cure due to differential strains or frictional forces between the part and the tooling on which it is manufactured. Aluminium or steel tools have much higher expansion coefficients than composites, and tend to stretch the parts as they heat up. This can happen as a result of small shear stresses at the tool interface sustained by autoclave pressure causing tension in the part. If the stresses are not uniform through the thickness, they can lead to distortion.[9] During stamp-forming of thermoplastic matrix composites, much larger pressures can be generated than those seen in shaping thermoset matrix prepregs, leading to potentially very high frictional shear and associated residual stresses.

A second tool-part interaction mechanism is due to locking, where the geometry of the part forces it to move with the tool as it expands. The simplest example is a filament wound tube, where substantial tensile stresses can be induced due to expansion of the mandrel. For example, Ganley *et al.* estimated stresses at the surface of 250 MPa for unidirectional IM7/977-2 carbon fibre-epoxy prepreg hoop wound on a steel mandrel,[10] which led to very large spring-in when the tubes were sliced longitudinally.

7.2.4 Other mechanisms

Moisture causes swelling of the matrix which produces similar effects to thermal or chemical volume changes, for example changing the curvature of unsymmetric laminates.[11]

Volume fraction variations through the thickness can arise, especially where there is resin bleed during the cure. These can produce distortion even in flat unidirectional composites.[12]

Fibre movement during the cure can cause changes in geometry and properties leading to stresses and distortion. Consolidation and resin flow at radii can lead to corner thickening with concave tooling and corner thinning with convex tooling,[13] and the effect is especially pronounced with tooling that contains both concave and convex regions close to each other. This can cause volume fraction variations and resin-rich regions which produce distortion. Wrinkles that can arise at corners, particularly with convex tooling, and separation between the part and tool may also affect residual stress development. Differential curing through the thickness due to temperature lags and exotherms can be important in thick parts, and may cause additional residual stresses and gradients through the thickness.[14]

7.3   Distortion in flat parts

7.3.1 Distortion due to asymmetric layups

If the layup is not symmetric, then the differential contractions during cooldown can produce deformation of the laminate. The classic example of this phenomenon is a (0/90) unsymmetric laminate, which will deform into a circular arc, as shown in Fig. 7.4. A (45/–45) laminate will twist on cooldown, whilst more complicated asymmetric laminates will exhibit combinations of bending and twisting.

Experiments with carbon-epoxy have shown that the development of curvature with temperature is approximately linear,[15] and the distortion can be predicted quite accurately based on the room temperature thermoelastic proper-ties and the difference between the cure temperature and room temperature. If the glass transition temperature is below the cure temperature, then curvature
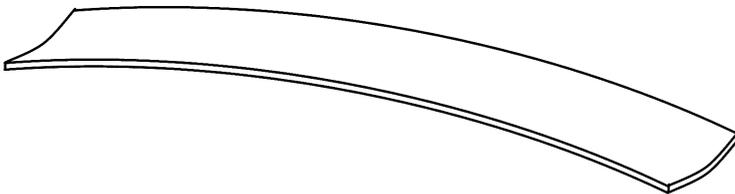
7.4 Curvature in (0/90) unsymmetric laminate due to residual thermal stresses.
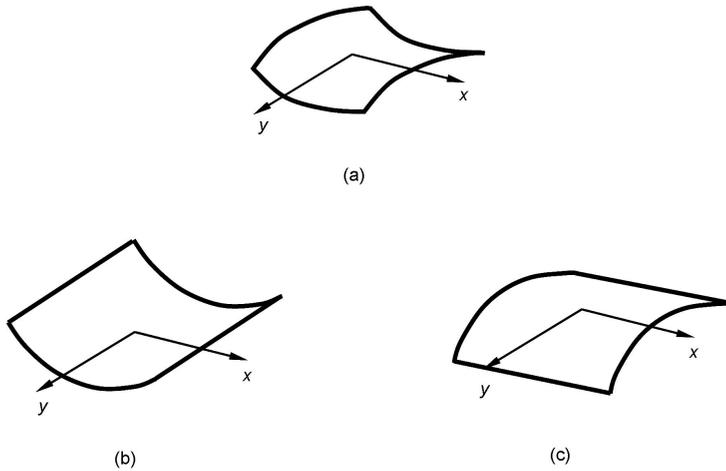
7.5 Initial saddle shape of (0/90) unsymmetric laminate (a) becomes unstable and switches to one of two stable cylindrical shapes (b) or (c).

only develops from that point until room temperature. Distortion will tend to reduce with time due to uptake of moisture, which causes a compensating swelling of the resin.

The deformation of even a simple flat (0/90) unsymmetric laminate is in fact quite complex. When the length to thickness ratio is small, a saddle shape is formed, with equal and opposite curvatures in the two directions. However, as this ratio increases, the saddle shape becomes unstable, and changes to one of two energetically favourable cylindrical shapes, as shown in Fig. 7.5. The geometry can be snapped between these two stable states. Solutions based on the Rayleigh-Ritz technique are available to predict the resulting shape of simple plates.[16] Finite element techniques can also be used,[17] and are effective for more complex shapes.

Significant residual stresses are required to sustain these distortions, which is why they only arise on cooldown below the glass transition temperature. For the same reason chemical shrinkage does not usually contribute significantly to distortion due to asymmetric layups because it mainly occurs before vitrification. This has been demonstrated by experiments reheating cured (0/90) unsymmetric laminates of AS4/8552 carbon-epoxy. The laminates became flat at a temperature only slightly above the original cure temperature, indicating that most of the distortion was thermoelastic.[15]

7.3.2   Distortion due to resin bleed and volume fraction gradients

Flat plates are often observed to distort away from the tool with convex up curvature, especially when they are relatively thin. One mechanism that can

Resin-poor region on surface
(higher expansion coefficient)

Resin-rich region at tool
(lower expansion coefficient)
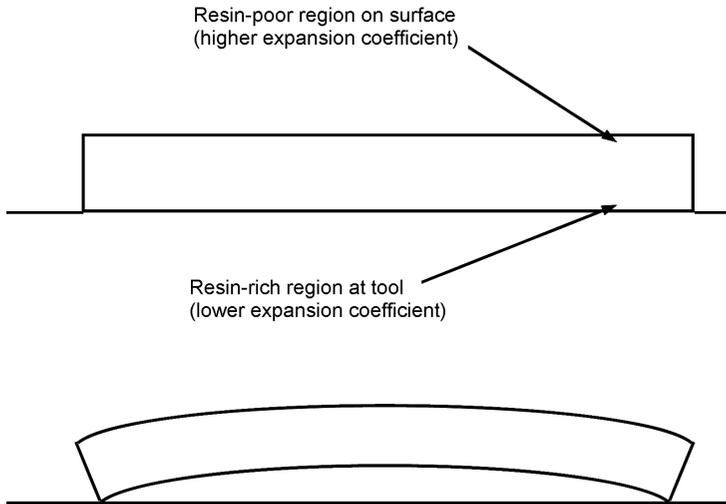
7.6 Distortion due to volume fraction gradient through the thickness.

cause this is variations of volume fraction through the thickness due to resin flow in materials with relatively low viscosity, or when resin is deliberately bled from the surface during consolidation. This can produce resin-poor regions at the surface, whilst near the tool interface, resin-rich layers can form. The thermal expansion coefficients increase with decreasing volume fraction and so tend to be higher on the tool side, leading to convex bowing during the cooldown from cure, as shown schematically in Fig. 7.6.

For example Radford reported bowing of 4 mm on 445 mm long T300/948A1 carbon-epoxy laminates 12 plies thick, and 70 mm bowing for 5-ply laminates 810 mm long.[12] Micrographs and fibre volume fraction measurements through the thickness showed a gradual gradient, but with marked differences in the surface plies. The bulk of the material had a fibre volume fraction between 48% and 52%, but on the surface ply it reached 58%, compared with only 41% for the ply in contact with the tool.

Expected curvatures were calculated using classical laminated plate theory based on measured volume fractions and thermoelastic properties derived from micromechanics, and gave similar magnitudes to the measured curvatures. Since the origin of this distortion is thermoelastic, it is reversible, and will decrease on reheating the part, or as moisture is absorbed.

7.3.3   Distortion due to tool-part interaction

An alternative mechanism that can cause bowing of flat laminates is tool-part interaction. Small shear stresses at the part surface due to tool expansion can build up over a long distance to cause significant tension in the part. If the part is
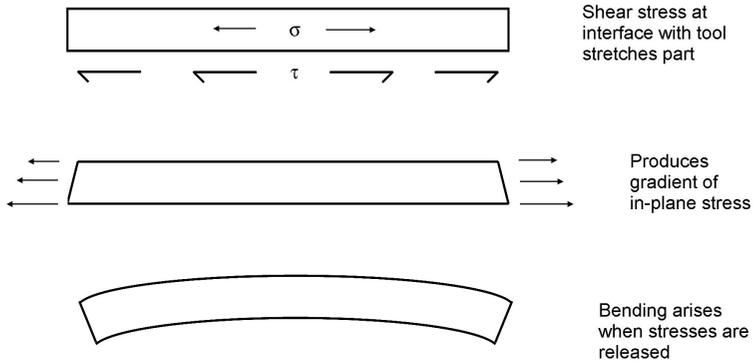
7.7 Distortion due to shear interaction at tool interface.

uniformly stretched, the stresses may be released after manufacture without causing any distortion. A variation of stress through the thickness is required to produce a change in shape. If a stress gradient arises in the part early in the cure, it will be locked in when vitrification occurs, causing bending when the stresses are released, as illustrated schematically in Fig. 7.7. In contrast to bowing caused by volume fraction gradients, this mechanism is non-thermoelastic, and so is not affected by subsequent temperature changes.

Stresses arising due to tool-part interaction have been measured on flat strips of unidirectional AS4/8552 prepreg 650 mm long, and one-ply thick (0.25 mm) cured on an aluminium base plate with a layer of FEP release film.[18] Spots of the prepreg were precured and strain gauges bonded, allowing strains to be measured throughout the standard autoclave cure cycle with dwells at 120ºC and 180ºC. Figure 7.8 shows the results.
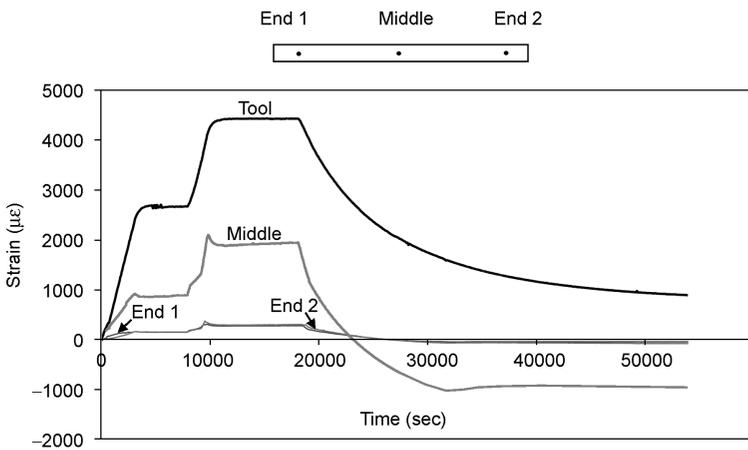
7.8 Strains on flat unidirectional strips during the cure.[18]

Strains started to develop straight away, with about 900 microstrain in the first dwell, before gelation. The thermal expansion coefficient in the fibre direction is very small, so this indicates tensile stresses are developing, with a magnitude of about 120 MPa. This is apparently a result of friction between fibres and the tool as the resin is effectively a liquid and would not be expected to transfer any significant stress before gelation. The readings from the gauges near the ends of the strip showed that stress builds up approximately linearly, with a shear stress of around 0.1 MPa at the tool surface. The strain continued to increase, reaching about 2000 microstrain after vitrification on the second dwell, corresponding to about 250 MPa, and an equivalent shear stress of approximately 0.2 MPa. This is a very high stress at a point in the cure when the material is normally assumed to be stress free. Strips with four unidirectional plies of the same material with the strain gauges attached to cured spots on the top ply showed about a quarter of the strain of the single-ply case, confirming that stresses are due to a constant shear stress at the tool-part interface. Similarly high stresses induced by tool-part interaction have been inferred from experiments with an instrumented tool plate.[19]

The stresses in these flat plates did not lead to significant bowing, presumably because they were fairly uniformly distributed through the thickness. However, if stress gradients arise through the thickness, they can produce considerable distortion. For example Twigg *et al.* measured convex up bowing of up to 40 mm on 1200 mm long flat unidirectional T800H/3900-2 carbon-epoxy plates four plies thick, which was attributed to tensile stresses near the tool surface decaying through the thickness.[9]

One reason for a stress gradient is frictional effects before gelation. Twigg *et al.* postulated that the inter-ply friction coefficient in their material is less than the friction coefficient between the tool and part.[9] This means that stresses in the surface fibres will not all be transferred through the thickness, giving rise to a stress gradient and curvature. In contrast ply pull-out tests on AS4/8552 subjected to the same process conditions as the autoclaved laminates showed a higher resistance to shear before gelation between layers of prepreg than between prepreg and aluminium.[20] This scenario would not give rise to a stress gradient, and is consistent with the low level of bowing seen on the flat plates of that material.[18]

The layup can have a significant effect on the stresses built up before gelation. Although unidirectional flat plates of AS4/8552 did not bow, similar tests with a $(0/90)_s$ layup on specimens 1000×50 mm produced a consistent convex up curvature, with a maximum bowing of about 8 mm.[21] This compares with maximum bowing within the range -2 to $+2$ mm for unidirectional specimens of the same dimensions manufactured in the same way. The difference is believed to be because only the surface 0° ply carries the full tension induced by shear at the tool before gelation. These stresses cannot all be transferred through the 90° ply, because the fibres more easily slip over each

other in this direction, and the effective frictional shear stress is reduced. There is therefore a stress gradient through the thickness, resulting in curvature.

This mechanism has been modelled by Bapanapalli and Smith in a finite element simulation assuming that a surface layer of material of constant thickness is subject to a certain tensile strain.[22] The thickness and strain parameters were deduced by fitting the curvature results of unidirectional strips of different thicknesses, and these values were then used to predict the curvatures of cross-ply specimens of different layups and thicknesses, giving good correlation. Very different values of both parameters were required to fit results for Invar and aluminium tools. The material used was T800HB/3900-2, which gave significant curvatures for both unidirectional and cross-ply layups. However, the same approach would not be expected to predict the curvatures of AS4/8552 due to the different behaviour of the pre-preg, as discussed above. This illustrates the difficulties of modelling cure distortions, due to the number of interacting factors that control the response.

7.4   Spring-in of curved parts

7.4.1   Thermoelastic spring-in

The higher through-thickness expansion coefficient of composites such as carbon-epoxy compared with the in-plane expansion coefficients causes curved composites to spring-in on cooldown from cure. The effect is reversible, with the spring-in reducing if the part is reheated, and is referred to as thermoelastic spring-in. The magnitude can be predicted from the equation:

$$\frac{\Delta\theta}{\theta} = (\alpha_I - \alpha_T)\Delta T \qquad\qquad 7.1$$

where $\Delta\theta$ is the change in angle θ, α_I and α_T are the in-plane and through-thickness expansion coefficients and ΔT is the change in temperature.

This mechanism can be demonstrated from measurements on unidirectional and cross-plied L shaped parts heated in an oven.[23] AS4/8552 carbon-epoxy with a lay-up of 0_4 and a thickness of 1 mm was laid up and cured on the inside of an Invar tool with radius 20 mm, where the 0º direction follows the curvature. The width was 100 mm and arm length 100 mm. After cure, one arm was clamped to the base of the oven, and the change in the 90º angle was measured with the help of a laser reflected from a mirror on the other end of the specimen as it was heated.

Figure 7.9 shows the results for the angle as a function of temperature. The response is approximately linear, and the slope corresponds to a change in angle of 0.47º for a temperature change from 20º to 180º.

The in-plane expansion coefficient α_I from manufacturer's data was $0.02 \times 10^{-6}\,\mathrm{K}^{-1}$. The transverse coefficient α_T was measured independently to be
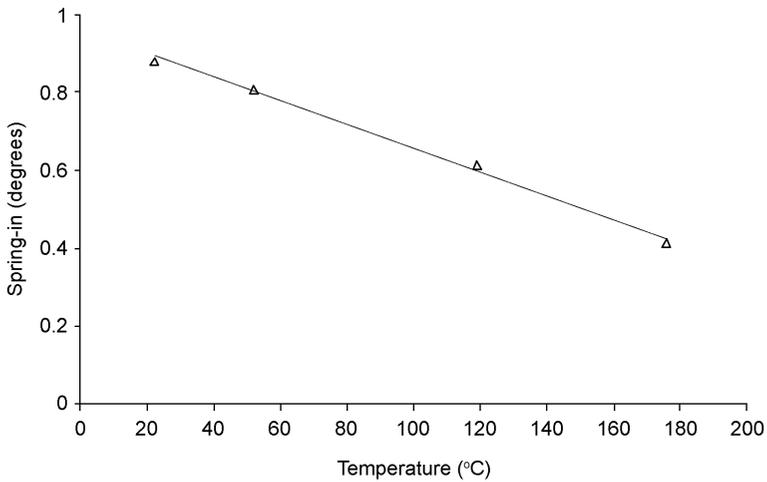
7.9 Thermoelastic response of unidirectional L specimens.[23]

$32.6 \times 10^{-6}\,\mathrm{K}^{-1}$ using strain gauges. Assuming transverse isotropy, and using this value for the through-thickness expansion coefficient in equation (7.1) gives a change in angle of 0.469°, the same as the measured result. Using laminated plate theory, the in-plane and through-thickness expansion coefficients for a $(0/90)_s$ cross-ply laminate were calculated to be $2.73 \times 10^{-6}\,\mathrm{K}^{-1}$ and $45.7 \times 10^{-6}\,\mathrm{K}^{-1}$ respectively. Putting these into equation (7.1) gives a predicted spring-in of 0.619°, which again was found to be very close to the measured value of 0.63°, confirming the validity of the thermoelastic calculations.

7.4.2   Chemical shrinkage after vitrification

Chemical shrinkage of the resin can be treated in the same way as thermal contraction, by adding an additional term to equation (7.1):

$$\frac{\Delta\theta}{\theta} = (\alpha_I - \alpha_T)\Delta T + (\phi_I - \phi_T) \qquad\qquad 7.2$$

where ϕ_I and ϕ_T are in-plane and through-thickness chemical shrinkages. This is a simplified version of the equation given by Radford and Rennick.[24] As discussed below, equation (7.2) is in fact only valid after vitrification, but can be used to calculate spring-in during this phase by taking ϕ_I and ϕ_T as the chemical shrinkage after vitrification. However, for many resins chemical shrinkage after vitrification is small. This was studied for AS4/8552 by measuring the curvatures of flat unsymmetric cross-ply laminates after interrupted cure cycles.[15] Specimens which were rapidly quenched just after the material vitrified showed similar final curvature to those quenched from the same temperature after the full cure cycle was completed. This shows that chemical shrinkage after

vitrification is negligible for this material, and would not be expected to contribute significantly to spring-in.

7.4.3   Spring-in due to shrinkage before vitrification

Most current models such as equation (7.2) do not distinguish between shrinkage before and after vitrification. However, in the phase between gelation and vitrification the composite is in a rubbery state, and can shear through the thickness. If it could shear freely, this would provide a mechanism to take up the change in circumferential length due to through-thickness contraction without inducing stresses in the fibre direction, eliminating any additional spring-in.

This is illustrated in Fig. 7.10. The schematics on the left show what happens when the material is stiff in shear, as it is when fully cured. With a through-thickness contraction while the part is constrained to the tool, there is no change in shape, and in-plane stresses are generated. When the part is released from the

Initial
shape at
gelation

Through-thickness
shrinkage during
cure

No shear – in-plane   Shears freely – no
stresses generated   residual stresses

Release from tool

Spring-in as residual   No spring-in, only shear
stresses released

(a) Stiff in shear   (b) Flexible in shear
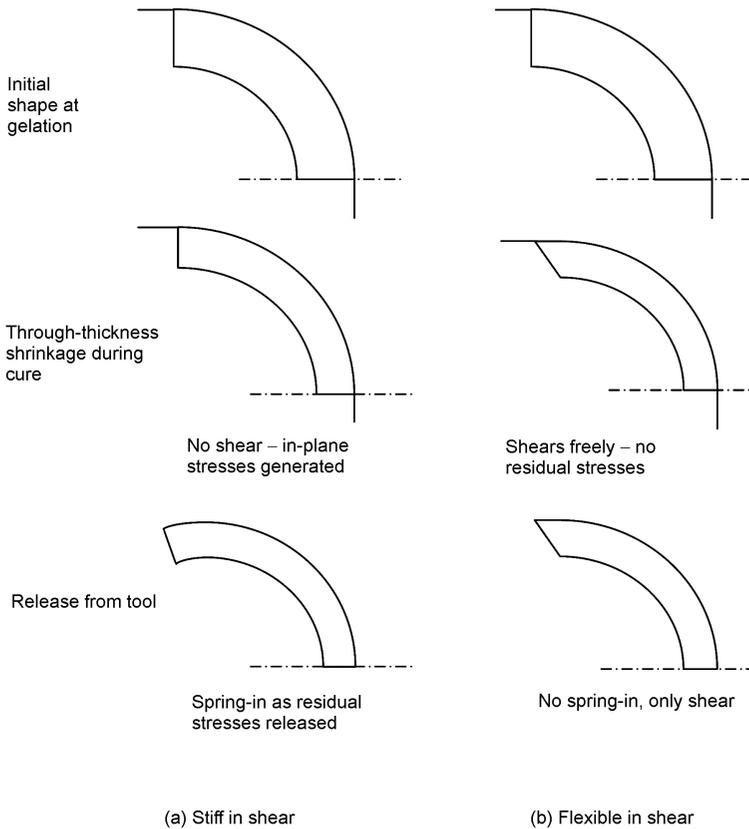
7.10 Change of angle due to a through-thickness contraction.

tool these stresses are released, and the part springs in. The schematics on the right illustrate the situation when the material is compliant in shear, as it is early in the cure. Now a through-thickness contraction leads to shearing of the part, with no in-plane stresses generated. There is therefore no spring-in, only through-thickness shearing.

In practice the material is not completely free to shear and this can be treated by a shear lag analysis.[25] If the rubbery shear modulus is high, or the composite is long compared with its thickness, the same result is obtained as with equation (7.2). However, as the shear modulus reduces, or as the length to thickness ratio decreases, the predicted amount of spring-in reduces.

Results are shown in Fig. 7.11 for AS4/8552 cross-ply laminates with different ratios of radius to thickness using a measured through-thickness shrinkage of 0.98%[26] and estimated through-thickness shear modulus of 43 MPa. The in-plane shrinkage was assumed to be negligible. When the thickness is large compared with the radius, the specimen is able to shear, and the predicted spring-in approaches the thermoelastic value of 0.62° given by equation (7.1). As the thickness becomes small compared with the radius, the predicted spring-in approaches the value of 1.50° given by equation (7.2).

This effect has been demonstrated experimentally by measuring spring-in of segments of 270° of cross-plied $(0/90)_{ns}$ AS4/8552 tubes from 1 to 4 mm thick. They were cured using a pressure bag simulating autoclave conditions on the inside of a 50 mm internal diameter carbon-fibre tube to eliminate any effects due to tool interaction.

The outer diameters of the composite parts were measured at room temperature and equivalent spring-in angles were calculated for a 90° angle with respect to the tube inner diameter measured at 180°C. The results confirm
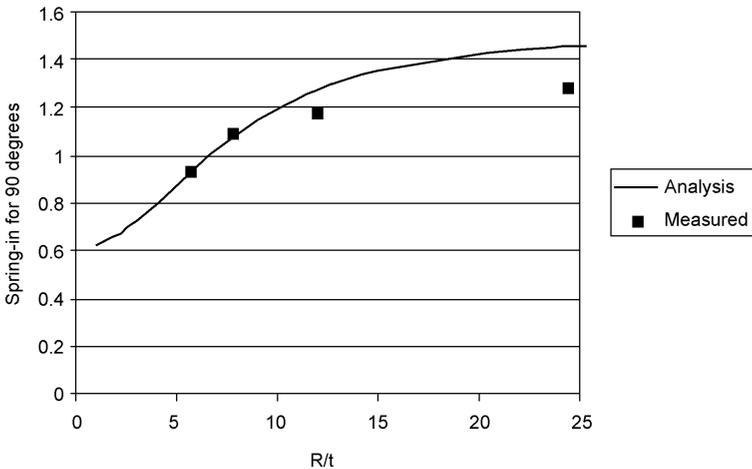
7.11 Shear lag effect on spring-in for different thickness curved cross-ply sections.

the predicted trend of reducing spring-in with increasing thickness, with values varying from 1.28º at 1 mm thickness to 0.93º at 4 mm. The shear lag analysis correlates quite well with the experimental results.

It is the total change in through-thickness strain between gelation and vitrification that controls spring-in during this phase, including thermal effects. If gelation occurs at a lower temperature than vitrification, there will be a through-thickness expansion on heating up to vitrification which will reduce the effect of chemical shrinkage. Both these components were included in the experimental value of shrinkage quoted here. Note that shrinkage before gelation will not contribute to this particular mechanism since the part geometry is only fixed when the resin gels.

When a curved section continues into adjacent flat sections such as with an L-shaped geometry, then the flat sections will have a similar constraining effect to a longer arc length, increasing the predicted spring-in towards the value given by equation (7.2). The resulting strain gradients in the flat sections will also cause further distortion due to bowing of the arms, complicating the deformed shape and making simple comparisons of spring-in angles difficult.

7.4.4   Spring-in due to fibre wrinkling and tool-part interaction

As discussed in Section 7.3.3, the higher thermal expansion of many tool materials compared with the composite causes the tool to stretch the part. If a stress gradient arises through the thickness, it will produce distortion that could either increase or decrease spring-in, depending which side the tooling is. However, on a curved part, there is a further effect as the stretching from the tool can interact with wrinkles formed in the curved sections. When prepreg is laid up around a radius, the path difference between inner and outer surfaces leads to fibre wrinkling on the inner surface such that any tool-part interaction stresses will be disproportionately carried by the fibres on the outside of the radius. This stress gradient opposes the effects of the other spring-in mechanisms, and can even cause spring-out in very thin parts.

This is illustrated by the results from the unidirectional L specimens with different thicknesses mentioned in Section 7.4.1. As well as the thermoelastic response, the total spring-in angles were measured with the help of a coordinate measurement machine.[21] Straight lines were fitted to the data from points at the ends of the radius to the ends of the arms to avoid the influence of arm bowing. Results are shown in Fig. 7.12 for specimens from 4 mm to 0.5 mm thick. The two thicker specimens gave similar results, but the 1 mm one showed a reduction in spring-in, whilst the 0.5 mm specimen actually sprang out. A similar trend was observed with cross-ply samples, although the magnitude of the effect was reduced.

The tool material was Invar, which still expands sufficiently to produce significant tool-part interaction. An even larger effect was found with an
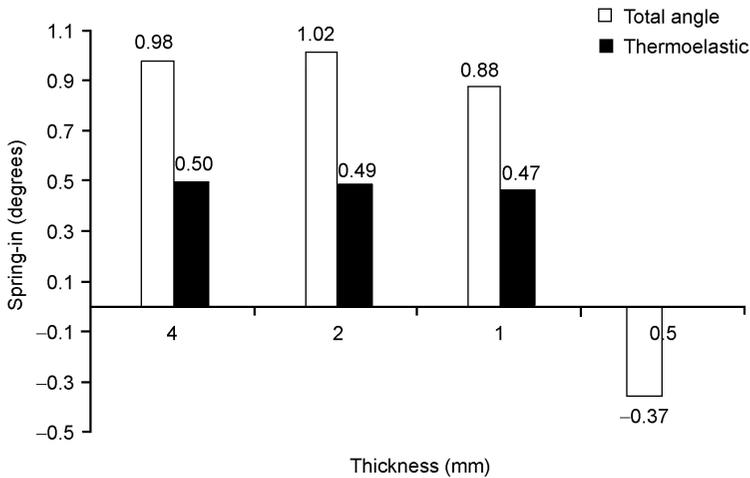
7.12 Effect of thickness on spring-in of unidirectional L sections.[23]

aluminium tool, with spring-out of as much as 16° measured in single-ply L sections. Note that this trend of reducing spring-in for thin parts is the opposite to that due to shear lag discussed in Section 7.4.3.

These effects have been analysed using a simple analytical model assuming the material at the surface expands with the tool, but that there is a linear stress gradient through the thickness.[27] The extent of the gradient was deduced from the kinematics of the change in circumferential length arising from the varying radius through the thickness when the plies are laid up in the corner. The analysis was able to explain the observed trends and give the approximate magnitude of the effect.

7.4.5   Effect of consolidation on spring-in

Consolidation due to resin flow and cure shrinkage prior to gelation causes reductions in thickness. The inextensible fibres tend to reduce this effect in curved sections cured on concave tooling, leading to higher corner thickness in the absence of ply-ply slip. This change of geometry can cause a small increase in thermoelastic spring-in, as can be seen from the results in Fig. 7.12. L sections 4 mm thick with corner thickening gave a thermoelastic spring-in of 0.50° compared with 0.47° for similar parts only 1 mm thick with relatively constant thickness. Although this is a fairly small effect, it was consistent. Cross-ply specimens with layup $(0/90)_{ns}$ exhibited a similar increase in spring-in from 0.63° at 1 mm thickness to 0.67° at 4 mm.

This difference can be predicted by finite element analysis taking account of the different geometry and volume fractions. Figure 7.13 shows a model used for this,[23] where the inner radius was increased to reproduce the corner thickness

50 mm

Corner thickening effect was simulated
by increasing the inner radii

Centre of the new arc was always
placed at the symmetry line

Symmetry line
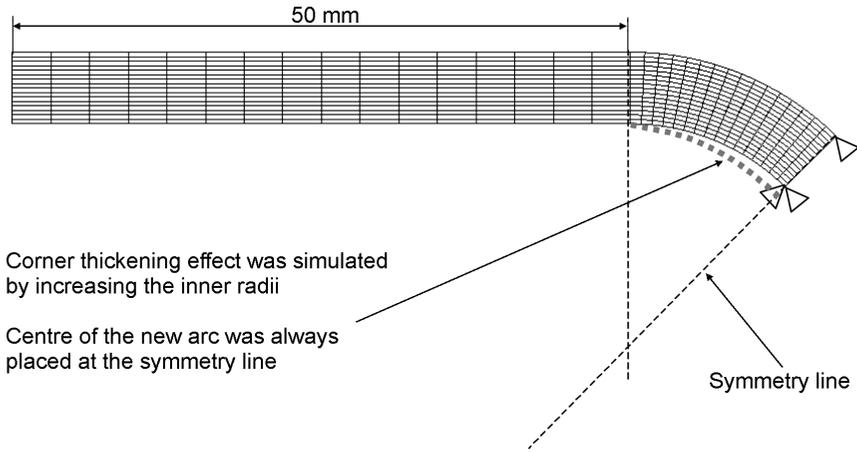
7.13 Finite element model of the effect of corner thickening on spring-in.[23]

measured experimentally. Material properties were adjusted for the change in volume fraction using micromechanics equations and assuming the thickness change was accompanied by resin flow into the corner. The results showed an increase in predicted spring-in from 0.47º to 0.49º for unidirectional material and from 0.62º to 0.65º for cross-ply, close to the measured values. The resin flow into the thickened corner can cause thinning of the adjacent laminate which may also have an influence on the distortion.

There are also other more complex effects due to consolidation which are still not properly understood. For example, stresses may be set-up due to the autoclave pressure on inside radii being reacted by tension in the fibres, which can contribute to spring-in. Separation between the part and tool may occur in the corner despite the autoclave pressure, and can increase spring-in.

7.5   Distortion in more complex parts

The same mechanisms discussed above can cause more complex distortions in larger scale structures. For example, measurements on long C-shaped components showed that in addition to the expected spring-in, there was twist along the length of the channel, which was attributed to tool-part interaction causing tension in the surface 45º ply.[21] There was also bowing of the web, which was again attributed to tool-part interaction.

Where the geometry of the part causes it to lock to the tool, high stresses can be generated, which can cause large distortions where stress gradients are present. For example, substantial distortion has been demonstrated in tests where a single ply of prepreg was wound around an aluminium tool to force inter-action.[28] Tensile stresses cause bending near the corners because of wrinkling, which means most of the load is carried in the straighter fibres on the outside. In

Aluminium   Prepreg ply wrapped around tool

Shape after removal from tool (approx. to scale)
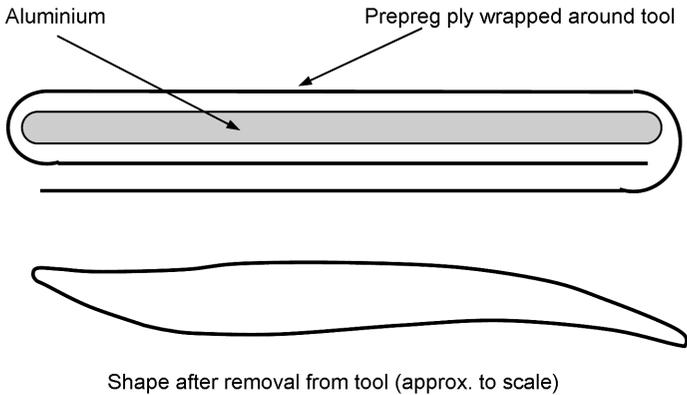
7.14 Schematic of distortion due to forced interaction with tool.[28]

addition, where the ply overlaps, there is a large stress gradient caused by the change in neutral axis. These effects produced the complex distortion shown in Fig. 7.14, with up to about 30 mm deflection on a part 500 mm long. Dropped plies in tapered layups similarly cause bending if there is tension from tool-part interaction. Analagous effects due to the part locking to the tool can be caused by the shape of the component, for example with features such as joggles or steps.[28] In these regions the influence of the fibre wrinkling effect depends on the extent to which the reversal of corner curvature leads to the reduction of wrinkling. These effects are rather complex and appear to depend, for example, on the quality of layup and fit of reinforcement to the tool.

Constraint between deformations of different parts of built-up structures can cause more complex distortions. For example, in a curved C spar with web stiffeners, the curved sections will tend to spring-in, but will be prevented from doing so by the stiffeners.[29] The shape arising can be analysed by finite element modelling including the mechanisms of thermal stress, cure shrinkage and tooling constraint. Other sophisticated finite element programs have been developed specifically for analysing manufacturing distortion, such as COMPRO,[30] which allows the whole process to be simulated including heat transfer, cure kinetics, resin flow, tool-interaction and residual stress development. This can model in detail the deformations induced in 2-D sections, and has also been used successfully in conjunction with 3-D models to simulate distortion in complex aircraft parts such as the T-45 box rib and 777 trailing edge fairing sandwich structures.[31]

Where large deformations of the material occur during forming of highly shaped parts, significant changes in fibre angles occur, which can greatly change the thermoelastic material constants and hence the residual stresses and distortions. Temperature gradients may also occur, which again can influence part distortion. These mechanisms have been successfully modelled by finite element simulation of parts formed on square and cylindrically shaped punch

tools, and an automotive body panel.[32] Similar effects have been seen on thermoplastic parts stamped out using rubber pad forming.[33]

Lastly, whilst the research emphasis has rightly been on understanding the causes of process-induced deformations and residual stresses there is also the potential for deliberately inducing residual stress and distortion states to achieve specific ends such as a multiplicity of stable geometries.[34]

7.6   Conclusions

The mechanisms causing distortion during the cure have been discussed, the most important being differential thermal contraction during cooldown, cure shrinkage and tool-part interaction. Distortion of flat plates due to asymmetric layups can be satisfactorily predicted from laminated plate analysis, with the contribution from chemical shrinkage usually being small. Where resin bleed occurs there can be significant changes of volume fraction through the thickness, and the effect of these on distortion can also be analysed with laminated plate theory. Thermal expansion of the tool can cause tensile stresses in the surface of the part leading to bowing away from the tool. This is harder to predict because it depends on the gradient of stress through the thickness, which is a function of the frictional behaviour of the material at the tool surface and between plies of different orientations.

Curved parts exhibit a thermoelastic spring-in on cooldown that can be predicted using laminated plate theory. In addition there is a non-thermoelastic component of spring-in due to shrinkage occurring primarily between gelation and vitrification. This depends on the way the material shears through the thickness, and so is a function of the constraint due to part geometry and ratio of in-plane dimensions to thickness as well as material properties. It can be predicted for simple curved geometry, but its effect on real parts is much more complex. Tool-part interaction can cause further distortion that can either increase or decrease spring-in, depending which side the tooling is on. This can interact with the effect of fibre wrinkling on the inside of the radius, causing a stress gradient through the thickness which tends to reduce the spring-in angle, and can even cause spring-out in very thin parts. Corner thickening associated with consolidation tends to slightly increase spring-in.

The same mechanisms are responsible for distortions in larger scale structures, with the constraint between different parts that tend to distort differently being crucial. Tool-part interaction mechanisms, in particular, can become complex due to features of the geometry causing the part to lock to the tool. Some successes have been achieved in modelling distortions of more complicated parts, but there is still a need for further understanding of the mechanisms and advances in the analysis tools before the behaviour of real components can be predicted with confidence.

7.7   References

1. Nedele, M. and Wisnom, M. R., Micromechanical modelling of a unidirectional carbon fibre reinforced epoxy composite subjected to mechanical and thermal loading, *Proc. American Society for Composites Seventh Technical Conference, Pennsylvania State University*, pp 328-338, October 1992.

2. Hyer, M. W., Some observations on the cured shape of thin unsymmetric laminates, *Journal of Composite Materials* 15:175–194, 1981.

3. Kim, K. S. and Hahn, H. T., Residual stress development during processing of graphite/epoxy composites, *Composites Science and Technology* 36:121, 1989.

4. Hyer, M. W., Rousseau, C. Q. and Tomkins, S. S., Thermally induced twist in graphite-epoxy tubes, *Journal of Engineering Materials and Technology* 110:83–88, 1988.

5. Nelson, R. H. and Cairns, D. S., Prediction of dimensional changes in composite laminates during cure, *34th International SAMPE Symposium* pp 2397–2410, May 1989.

6. Wisnom, M. R., Gigliotti, M., Ersoy, N., Campbell, M. and Potter, K. D., Mechanisms generating residual stresses and distortion during manufacture of polymermatrix composite structures, *Composites Part A*, 37:522–529, 2006.

7. Li, C., Potter, K. D., Wisnom, M. R. and Stringer, L. G., In-situ measurement of chemical shrinkage of MY750 epoxy resin by a novel gravimetric method, *Composites Science and Technology* 64:55–64, 2004.

8. Unger, W. J. and Hansen, J. S., The effect of cooling rate and annealing on residual-stress development in graphite fiber reinforced peek laminates, *Journal of Composite Materials* 27:108–137, 1993.

9. Twigg, G., Poursartip, A. and Fernlund, G., Tool-part interaction in composites processing Part I: experimental investigation and analytical model, *Composites* 35A:121–133, 2004.

10. Ganley, J. M., Maji, A. K. and Huybrechts, S., Explaining spring-in in filament wound carbon fiber/epoxy composites, *Journal of Composite Materials* 34:1216–1239, 2000.

11. Wu, Y. J., Takatoya, T., Chung, K., Seferis, J. C. and Ahn, K., Development of the transient simulated laminate (TSL) methodology for moisture ingression studies using unsymmetric laminates, *Journal of Composite Materials* 34:1998–2015, 2000.

12. Radford, D. W., Cure shrinkage-induced warpage in flat uniaxial composites, *Journal of Composites Technology & Research* 15:290–296, 1993.

13. Hubert, P. and Poursartip, A., Aspects of the compaction of composite angle laminates: An experimental investigation, *Journal of Composite Materials* 35:2–26, 2001.

14. Bogetti, T. A. and Gillespie, J. W., Process-induced stress and deformation in thick-section thermoset composite laminates, *Journal of Composite Materials* 26:626–660, 1992.

15. Gigliotti, M., Wisnom, M. R. and Potter, K. D., Development of curvature during the cure of AS4/8552 [0/90] unsymmetric composite plates, *Composites Science and Technology* 63:187–197, 2003.

16. Dano M. L. and Hyer M. W., Snap-through of unsymmetric fiber reinforced composite laminates, *International Journal of Solids and Structures* 39:175–198, 2002.

17. Gigliotti, M., Wisnom, M. R. and Potter, K. D., Loss of bifurcation and multiple shapes of thin [0/90] unsymmetric composite plates subject to thermal stress, *Composites Science and Technology* 64:109–128, 2004.

18. Potter, K. D. Campbell, M. and Wisnom, M. R, Investigation of tool/part interaction

effects in the manufacture of composite components, *14th International Conference on Composite Materials, San Diego*, July 2003.

19. Twigg, G., Poursartip, A. and Fernlund, G., An experimental method for quantifying tool-part shear interaction during composites processing, *Composites Science and Technology* 63:1985–2002, 2003.

20. Ersoy, N., Potter, K. and Wisnom, M. R., An experimental method to study the frictional processes during composites manufacturing, *Composites Part A* 36:1536–1544, 2005.

21. Garstka, T., Ersoy, N., Potter, K. and Wisnom, M. R., The effect of tool-part interaction on the shape of curved composite laminates, to be published.

22. Bapanapalli, S. K. and Smith, L. V., A linear finite element model to predict processing-induced distortion in FRP laminates, *Composites Part A* 36:1666–1674, 2005.

23. Garstka, T., Potter, K. and Wisnom, M. R., Thermally induced spring-in in composite L-shaped and U-shaped laminates, to be published.

24. Radford, D. W. and Rennick, T. S., Separating sources of manufacturing distortion in laminated composites, *Journal of Reinforced Plastics and Composites* 19:621–641, 2000.

25. Wisnom, M. R., Ersoy, N. and Potter, K. D., Shear lag analysis of the effect of thickness on spring-in of curved composites, *Journal of Composite Materials*, in press, 2006.

26. Garstka, T., Ersoy, N. and Potter, K. D., In-situ measurements of through-the-thickness strains during processing of AS4/8552 composite, *Composites Part A*, submitted.

27. Garstka,T., C. Langer, K. D. Potter and M. R. Wisnom, Combined effect of tool-part interaction and fibre wrinkling on the shape of curved laminates, *Proc. CANCOM, Vancouver*, August 2005.

28. Potter, K. D., Campbell, M., Langer, C. and Wisnom, M. R., The generation of geometrical deformations due to tool/part interaction in the manufacture of composite components, *Composites Part A*, 36A:301–308, 2005.

29. Svanberg, J. M., Altkvist, C. and Nyman, T., Prediction of shape distortions for a curved composite C-spar, *Journal of Reinforced Plastics and Composites* 24:323–339, 2005.

30. Johnston, A., Vaziri, R. and Poursartip, A., A plane strain model for process-induced deformation of laminated composite structures, *Journal of Composite Materials* 35:1435–1469, 2001.

31. Fernlund, G., Osooly, A., Poursartip, A., Vaziri, R., Courdji, R., Nelson, K., George, P., Hendrickson, L. and Griffith, J., Finite element based prediction of process-induced deformation of autoclaved composite structures using 2D process analysis and 3D structural analysis, *Composite Structures* 62:223–234, 2003.

32. Hsiao, S. W. and Kikuchi, N., Numerical analysis and optimal design of composite thermoforming process, *Computer Methods in Applied Mechanics and Engineering* 177:1–34, 1999.

33. Wijskamp, S. and Akkerman, R., Tool-part interaction during rubber forming of composites, *8th ESAFORM Conference On Material Forming, Cluj-Napoca, Romania*, April 27–29, 2005.

34. Potter, K. D. and Weaver, P. M., A concept for the generation of out-of-plane distortion from tailored FRP laminates, *Composites A* 35A, 1353–1361, 2005.